P260

CALIBRATION SYSTEM FOR ARM RADARS

Nitin Bharadwaj*, Kevin Widener, Andrei Lindenmaier, and Vijay Venkatesh
Pacific Northwest National Laboratory, Richland, WA.

1 INTRODUCTION

The Atmospheric Radiation Measurement (ARM) Climate Research Facility is a U.S. Department of Energy (DOE) user facility for the study of global and regional climate by the research community. The Atmospheric Radiation Measurement (Stokes and Schwartz, 1994; Ackerman and Stokes, 2003) program has been in the forefront of climate research for over two decades.The ARM facility has established a cloud and precipitation radar facility (Bharadwaj et al., 2011)to enable the observation of cloud and precipitation systems under various climate regimes. The purpose of the radars is to collect and maintain a comprehensive and continuous long-term data sets that provide observations of cloud and precipitation over a wide range of environmental conditions.

ARM has operated cloud profiling radars for over ten years and the data from these profiling radar has lead to the development of many retrieval techniques to characterize clouds. However, the profiling radar make observations in only two dimensions:namely, height and time. The scanning ARM radars are deployed at the four fixed ARM sites and at the two ARM mobile facilities. The four fixed ARM sites are the Southern Great Plains (SGP) site in Oklahoma, Northern Slopes Alaska (NSA) in Alaska, Tropical Western Pacific (TWP-Darwin) in Darwin, Australia, and Tropical Western Pacific (TWP-Manus) in Manus Island. The ARM mobile facility 1 (AMF1)and ARM mobile facility 2 (AMF2)are deployed around the world for targeted measurement campaigns. The scanning radars include high powered C-band, X-band precipitation radars; and two dual-frequency scanning radars operating at X/Ka-band and Ka/W-band respectively. All of ARM's scanning radars are unattended 24/7 operational radars that are remotely monitored and operated via the internet.

The scanning cloud radars will be operated in pairs as dual-frequency radars with scanning controlled by a single pedestal. This single pedestal configuration enables simultaneous observations of the cloud field with two widely separated frequencies. Figure 1 shows the SACRs deployed by the ARM climate research facility. The principles and applications described in this paper are applicable to X-SACR, Ka-SACR and W-SACR. However, this paper will limit the description to Ka-SACR for brevity. The specifications of SACR systems shown in Fig. 1 are listed in Table 1. The Ka/W-SACR is a dual-frequency radar deployed at SGP, NSA and AMF1. The Ka/W-SACR consists of an Ka-band and W-band antenna mounted on a single pedestal to make dual-frequency observation of the cloud and precipitation. This paper presents a calibration system for the ARM radars that enable the calibration of the system using a trihedral corner reflector. A novel technique to counter the effect of receiver saturation from corner reflector is presented. The paper presents the errors in the calibration system for an operational framework. Data from the ARM radars will be presented highlighting the applicability of the method and its usefulness for unmanned radars deployed in in remote locations.

*Corresponding author address: Nitin Bharadwaj, 902 Battelle Blvd, MSIN K9-38 , Richland, WA-99352. Email: nitin@pnnl.gov

2 REFLECTIVITY CALIBRATION FOR VOLUME TARGETS

The equivalent reflectivity factor is estimated from the received power at the antenna reference plane as shown in Fig. 2. The equivalent reflectivity factor is given by

$$Z_e = C\bar{P}R^2 \tag{1}$$

In practice Z_e is expresses in mm^6m^{-3} (dBz in decibel scale). The radar equation can now be written as

$$Z_e\,[dBz] = \hat{P}_r\,[dBm] + C\,[dB] + 20\log\left(R\,[m]\right) \tag{2}$$

where $\hat{P}_r[dBm]$ is the power and the C is the radar constant estimated at antenna reference plane (see Fig. 2). Traditionally, the antenna reference plane is used to compute the radar constant and is given by

$$\begin{aligned} C \;=\; & 10\log\{\frac{1}{\pi^5|K_w|^2}\left(\frac{2}{c\tau}\right)\left[\frac{\left(4\pi^3\right)}{P_tG_0^2}\right]\left(\frac{8\ln 2}{\pi\theta_b\phi_b}\right) \\ & \lambda^2 10^{21}\ell_t\ell_r\ell_f\ell_d\ell_p\} \end{aligned} \tag{3}$$

In equation (3) the units conversion factor 10^{21} is the constant necessary to express the reflectivity in mm^6m^{-3}. All the parameters used in the radar equation are listed in Table 2 and the appropriate signal paths are shown in Fig. 2. The equivalent reflectivity factor for SACR is estimated from the power at the reference plane located at the input of the digital receiver, $\hat{P}_d$ (see Fig. 2). The radar constant

Table 1: Specification of ARM scanning radars

Parameter	W-SACR	Ka-SACR	X-SACR
Transmitter			
Type	EIKA	EIKA	TWTA
Center frequency (MHz)	93930	35290	9720
Peak power output (kW) 200	1.7	2.2	20
Duty cycle (%)	1.0	5.0	1.0
Max pulse width (μs)	1.5	13.0	40.0
Transmit polarization	H	H	H+V
Max PRF (kHz)	20.0	10.0	10.0
Antenna and Pedestal			
Antenna size (m)	0.9	1.82	1.82
3-dB Beam width (Deg)	0.30	0.33	1.20
Gain (dB)	54.5	53.5	42.3
Maximum scan rate (deg/s)	36.0	36.0	36.0
Receiver			
A/D (bits)	16	16	16
Receive polarization	H,V	H,V	H,V
Noise figure (dB)	6.0	5.0	4.5
Sampling rate (MHz)	120	120	120
Decimation factor	Adj	Adj	Adj
Video Bandwidth	Adj	Adj	Adj

H+V=Simultaneous horizontal and vertical polarization
H=Horizontal polarization and V=Vertical polarization

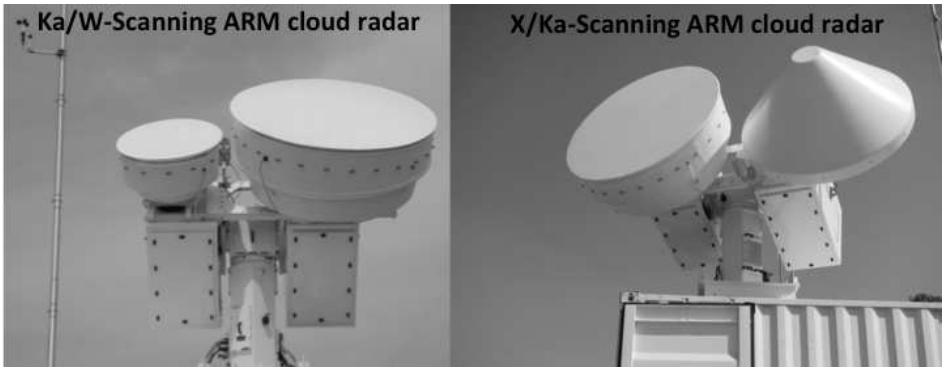

Figure 1: Photographs of scanning ARM cloud radars (SACR).

for SACR is computed using equation (3) as

$$C_{sacr}\,[dB] = C\,[dB] - G_r\,[dB]\,. \tag{4}$$

The receiver gain, G_r, is estimated using the noise source. The reflectivity factor is now computed as

$$Z_e\,[dBz] = \hat{P}_d\,[dBm] + C_{sacr}\,[dB] + 20\log\left(R\,[m]\right) \tag{5}$$

3 CORNER REFLECTOR BASED CALIBRATION

Trihedral reflectors are commonly used to routinely calibrate several types of radar systems. Triangular trihedral corner reflector is constructed with three triangular conducting planes oriented such that each section is perpendicular to the others. Figure 3 shows a trihedral reflector with triangular faces that is commonly used for the calibration of radars. The equivalent reflectivity factor can be estimated as a relative measurement using a standard corner reflector. The radar constant estimated from the corner reflector observations is given by

$$\begin{aligned} C_{cr} \quad = \quad & 10\log\{\frac{1}{\pi^5|K_w|^2}\left(\frac{2}{c\tau}\right)\left[\frac{8\ln 2}{\pi\theta_b\phi_b}\right]\left(\frac{\sigma_{cr}}{\hat{P}_{cr,d}R_{cr}^4}\right) \\ & \lambda^4 10^{18}\ell_f\ell_p\ell_n\}, \end{aligned} \tag{6}$$

where σ_{cr} is the radar cross-section of the corner reflector, $R-cr$ is the range to the corner reflector, and the other parameters are as listed in Table 2. The received power from the corner reflector, $\hat{P}_{cr,d}$, is measured at the reference plane at the digital receiver input. The reflectivity factor is

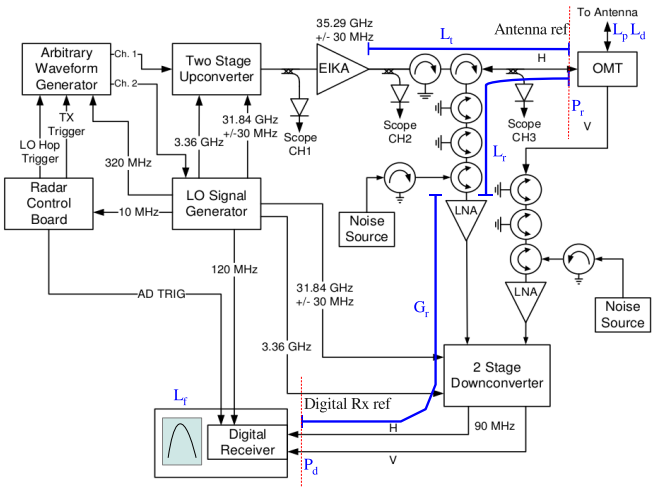

Figure 2: Block diagram of Ka-SACR illustrating the system design.

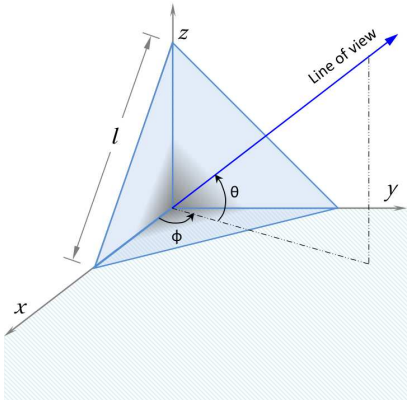

Figure 3: Illustration of the geometry of a triangular trihedral corner reflector. The line of view is the direction of the bore sight of the antenna beam with respect to the corner reflector.

computed as

$$Z_e\,[dBz] = \hat{P}_d\,[dBm] + C_{cr}\,[dB] + 20\log\left(R\,[m]\right). \quad (7)$$

As it can be observed the calibration constant $C_{cr}\,[dB]$ negates the used of well calibrated measurements of the radar subsystems such as the transmit power, antenna gain and RF path losses.

4 ERROR CONSIDERATION FOR OPERATIONS

There are several factors that must be taken into account while performing end-to-end calibration with a trihedral corner reflector. Some of most significant factors are discussed in the following sections.

Table 2: Parameters used for Ka-SACR Calibration

Parameter	Description
$\lvert K_w\rvert^2$	Dielectric factor
τ	Pulse width
P_t	Peak power
G_0	Antenna gain
θ_b	Beam width
ϕ_b	Beam width
λ	Wavelength
ℓ_t	Transmit loss
ℓ_r	Receive loss
ℓ_f	Finite bandwidth loss
ℓ_p	Probert-jones correction
ℓ_d	two-way radome loss
G_r	receiver gain

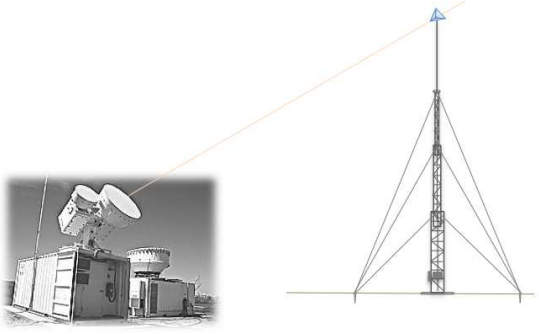

Figure 4: Illustration of the setup for calibration with a triangular trihedral corner reflector.

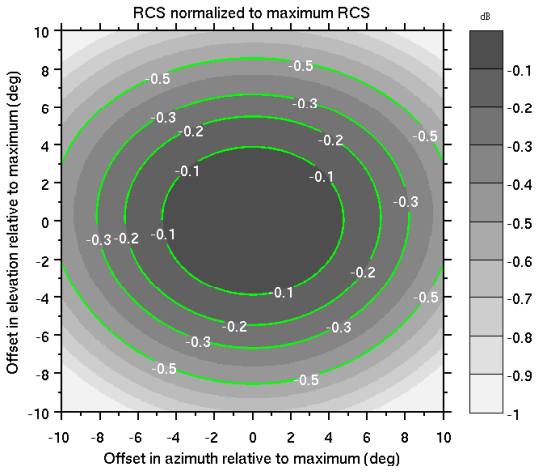

Figure 5: Reduction in RCS as a function of angular offset from bore-sight of the trihedral corner reflector.

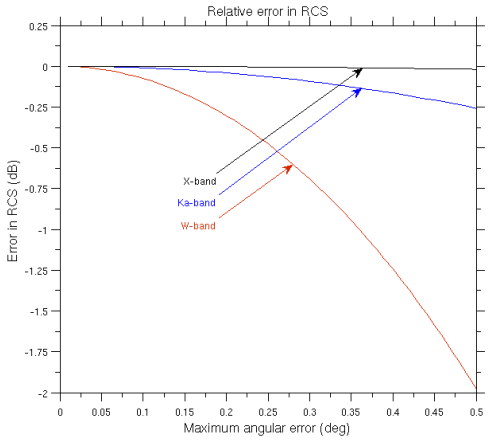

Figure 6: Error in RCS of trihedral corner reflector as a function of the angular error between the faces of the reflector.

4.1 Radar cross-section of corner reflector

The radar cross-section (RCS) of a trihedral corner reflector is a function of the view angle of the radar beam. The maximum radar cross-section for a reflector shown in Fig. 3 is given by

$$\sigma_{cr} = \frac{\pi \ell^4}{3\lambda^2} \tag{8}$$

The maximum radar cross-section in equation (8) occurs for a line of view corresponding to $\theta = 35.25°$ and $\phi = 45°$ which is the bore sight of the corner reflector. In practice it is not always possible to have a line of view to provide the maximum radar cross-section. The reduction in the RCS for offsets in the line of view is shown in Fig.5. The trihedral reflector has a very wide field of view and the reduction in RCS is small. The RCS reduction is within ± 0.2 dB for angular offsets less than $5.0°$. The RCS of the trihedral is affected by the angular errors between the faces of the trihedral. The angular error in the manufacturing of the trihedral reflector is defined as the maximum offset angle from the faces being orthogonal (i.e., $90°$). The error in RCS due to manufacturing errors is shown in Fig.6 for a 6.4-inch reflector for different frequencies (Craeye et al., 1997). With modern manufacturing methods the error in RCS is well within 0.1 dB. The errors in RCS are negligible for centimeter wavelength radars when compared to millimeter wavelength radars.

4.2 Transmitter and receiver configuration

The configuration of the transmit waveform and receiver is very important for performing calibration with a corner reflector. The key elements pertain to the nearest observable range gate and receiver saturation. The received signal from a corner reflector can be very strong which will saturate the receiver in most systems. The observation setup must include mechanisms to negate receiver saturation. Receiver saturation can be eliminated by the addition of fixed attenuators in the front end of the receiver or incorporate a system to lower the transmitter peak power.

The problem of receiver saturation in SACR, when observing corner reflector, is mitigated by reducing the peak power on the transmitted pulses. The amplitude of the waveform generated is scaled down to lower the drive power to the EIKA which in turn reduces the peak-power of the transmitter. However, it is important to measure the reduction in peak power due to scaling down of the waveform. Since SACR's are deployed at remote sites it is not possible to make field measurements for the operational corner reflector calibration scans that are routinely performed twice every day. An indirect technique is implemented to compute the reduction in peak power after scaling down the transmitted waveform. Observation of the corner reflector are made with the main lobe using a scaled waveform to avoid saturation. The reduction in power due to scaling is estimated by comparing the corner reflector observations made with the side-lobe at full power of the transmitter. Figure 7 shows the comparison of estimated power reduction obtained by using the novel method and field measurements. It can be observed that the indirect methods is in very good agreement with measurements using a calibrated power meter.

The use of pulse compression waveforms in systems using klystrons, TWTs and solid-state transmitters is becoming more common for precipitation and cloud radars. The use of pulse compression waveforms inherently puts a limitation on the location of the corner reflector because of the blind range issues related to the use long pulses. The corner reflector must be located beyond the blind range, which may be much farther than the optimal region for lo-

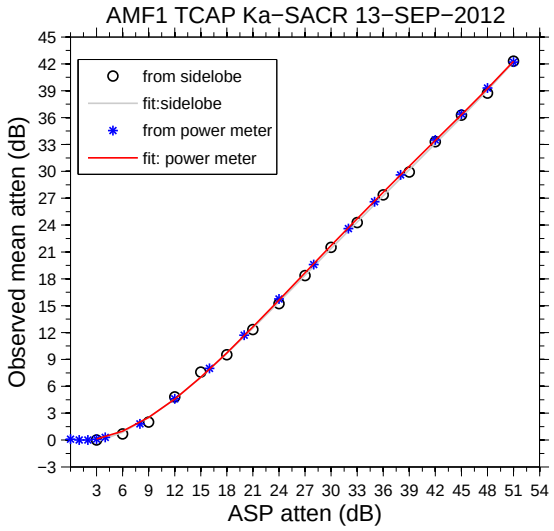

Figure 7: Reduction of peak-power by scaling the amplitude of the waveform generator. The results compare the power reduction measured using a power meter with the results obtained using an indirect method.

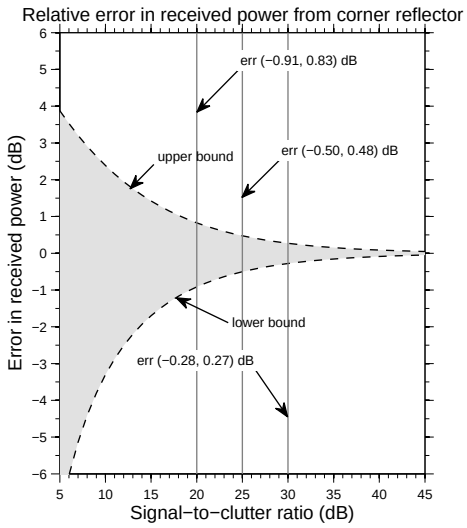

Figure 8: Bounds on the bias in received signal power from corner reflector as a function of signal-to-clutter ratio.

cating the reflector. The need for the corner reflector to be located closer to the radar is described in the following section.

4.3 Reflector location

The location of the reflector is very important to minimize the effect of ground clutter and multipath. The location of the corner reflector is primarily determined by the antenna beam width because the cross-range resolution degrades with range. The factors that must be taken into consideration for the location of the corner reflector are cross-range resolution, height of the reflector above ground and line of sight. The range to the reflector must be selected such that the beam size is small to avoid main-lobe clutter. If the beam is too wide the main-lobe clutter will be too strong and shall introduce a bias in the calibration. The height of the reflector is a function of the range and the requirements for the size of the tower becomes impractical if the reflector is too far. To avoid the need for a very large tower the reflector can be placed in the Fresnel region of the antenna pattern without significantly affecting the observations. The line of sight is defined in terms of the waveforms ability to only observe the corner reflector which means there should be no structures (towers, trees, buildings, etc.) within the volume of the pulse while observing the reflector. Therefore, corner reflector calibration has its limitations while using pulse compression waveforms with long pulses.

4.4 Signal-to-clutter ratio

The corner reflector calibration assumes the received power corresponds to the radar-cross-section of the reflector. However, in practice the received signal is contaminated by clutter signal. The clutter signals bias the calibration constant and the biases are depends on the signal-to-clutter ratio (SCR) and phase alignment of the signals. Figure 8 shows the bounds on the bias introduced due to the presence of ground clutter signal. It can be observed that the bias is on the order of 0.25 dB when the SCR is greater than 30 dB. Observations with and without the reflector can be made to access the signal-to-clutter ratio. Since both ground clutter and returns from the reflector have zero Doppler velocity tradition clutter filters cannot be applied to suppress ground clutter. Another approach is to have the reflector on a moving platform to introduce Doppler velocity on the received signal. Figure 9 shows the observations of the corner reflector region with and without the reflector on the tower. The observations are made with Ka-band Scanning ARM Cloud Radar (Ka-SACR), which operates with a 0.33 degree beam width. With a reflector size chosen to have adequate RCS for Ka-band it can be observed in Fig. 9 that SCR is sufficiently high to keep the bias within ± 0.25 dB.

4.5 Antenna pattern

In general, the data used in applications and retrievals are observations in the antenna far field. The corner reflector is located in the Fresnel region of the antenna pattern to mitigate some of the practical issues with beam size and tower heights. The observations of the corner reflector are made in the Fresnel region of the antenna pattern. The antenna beam shape is already well formed in the Fresnel region which is well beyond the near field of the antenna. The gain of the antenna is lower in the Fresnel region when compared to the far-field gain. The antenna pattern in the far field and Fresnel region for a circular aperture is sim-

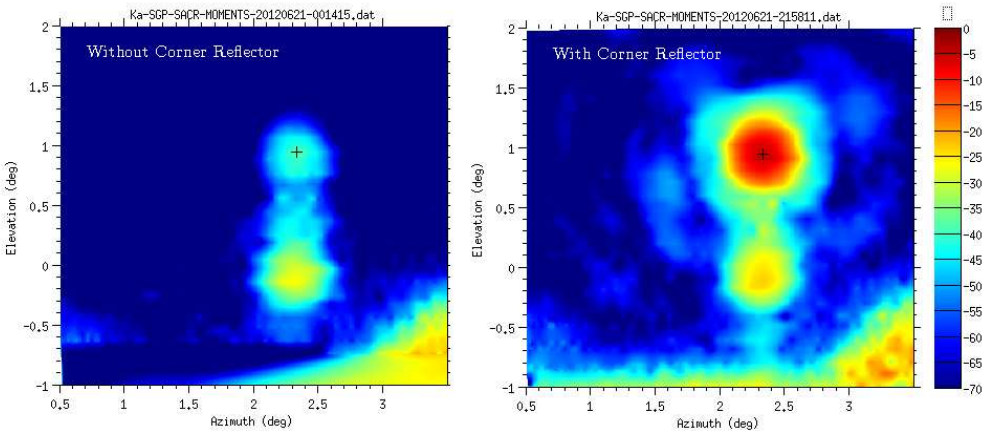

Figure 9: Received power (relative to corner reflector) of a 55 feet tower with and without a trihedral corner reflector. The observations were made with Ka-band Scanning ARM Cloud Radar (Ka-SACR).

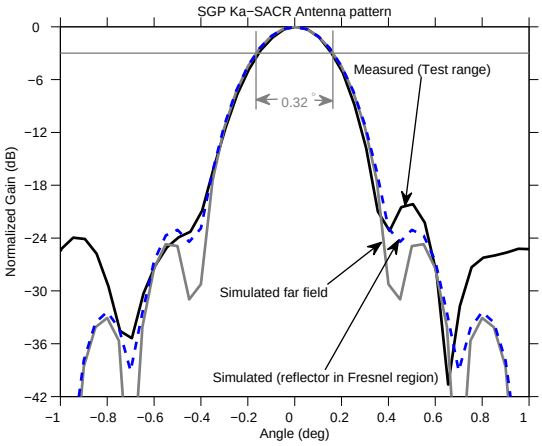

Figure 10: The antenna pattern of Ka-SACR from test range along with the simulated far field and Fresnel region antenna pattern.

ulated for Ka-SACR. The simulated patterns are shown in Fig. 10 along with the pattern measured in a test range. The Fresnel region pattern is simulated for a corner reflector located at about 460 m from the radar. It can be observed that the beam shape is well formed and closely matches the test range measurements in the main lobe of the antenna. The patterns shown in Fig. 10 are normalized to the gain. The gain of the antenna in the Fresnel region is computed numerically to obtain the correction for the received power. The correction is small as the reflector locations approach the far field of the antenna.

4.6 Environmental conditions

The environmental conditions in which the corner reflector observations are made have a significant impact on the usability of the data for calibration. The environmental conditions consist of three factors. One, the atmospheric state of the path between the radar and the reflector has a significant effect on the received power. At higher attenuating frequencies the presence of precipitation biases any calibrations done with a corner reflector. Two, the state of the surfaces on the corner reflector has an impact on the received power. The presence of layers of water or icing on the reflector surfaces changes the RCS and introduces larger uncertainties. Three, the state of the radome makes significant contribution to errors in calibration. Under condition of rain over radome, wet radome or icing on radome the received power from corner reflector cannot be used for calibration. Observations of corner reflector with data collected on a clear day are compared to data collected in a precipitating event in Fig. 11. The precipitating event most likely resulted in some form of icing on the radome due to wet snow and ice. The adverse effects of the environmental conditions are clear in Fig. 11. The received signal is attenuated by more than 20 dB compared to the data collected on a clear day. Corner reflector data should be used for calibration if and only if the data is collected under clear air conditions.

5 SUMMARY

Reflectivity calibration and tracking the calibration statefor long term observations is a critical component for cloud radars. Modernized radar systems are designed with built-in test equipment (BITE) to calibrate, track and monitor each sub-system. However, for an end-to-end system calibration the antenna must be included because the antenna pattern has a significant impact on the observations. An end-to-end system calibration methodology using corner reflector was presented and an analysis of error associated with the methodology was presented for operational consideration. A new method to mitigate the problem of receiver saturation was presented with validation based on field measurements. The corner reflector based calibration setup is a viable method for calibrating and maintaining calibration records for SACR.

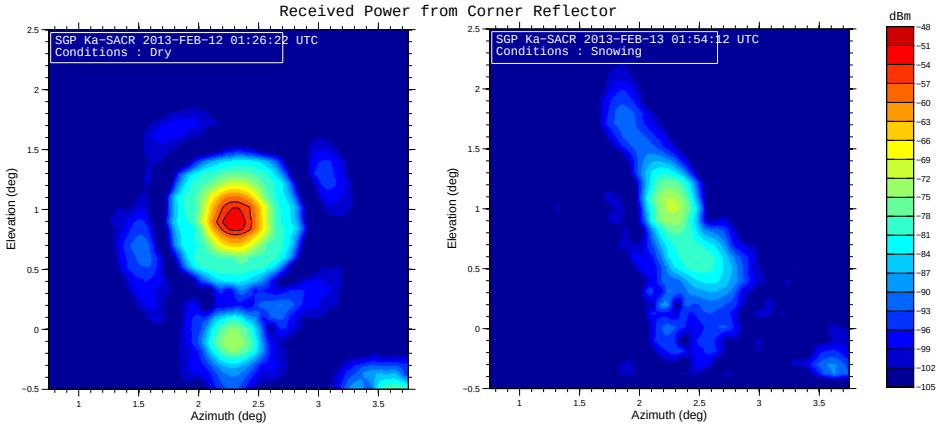

Figure 11: Comparison of corner reflector observations with and without precipitation.

ACKNOWLEDGEMENT

This research was supported by the Office of Biological and Environmental Research of the U.S. Department of Energy (under grant or contract number as part of the Atmospheric Radiation Measurement Climate Research Facility).

References

Ackerman, T. P. and G. M. Stokes, 2003: The atmospheric radiation measurement program. *Phys. Today*, **56**, 38–45.

Bharadwaj, N., K. B. Widener, K. Johnson, S. Collis, and A. Koontz, 2011: ARM radar infrastructure for global and regional climate study. *35 th Conf. on Radar Meteorology*, Amer. Meteor. Soc., Pittsburgh, PA, website.

Craeye, C. P., P. Sobieski, E. Robin, and A. guissard, 1997: Angular errors in trihedrals used for radar calibrations. *International Journal of Remote Sensing*, **18**, 2683–2689.

Stokes, G. M. and S. E. Schwartz, 1994: The atmospheric radiation measurement (ARM) program:programmatic background and design of the cloud and radiation testbed. *Bull. Amer. Meteor. Soc.*, **75**, 1201–1221.